Autoresonant (nonstationary) excitation of a collective nonlinear mode

J. Fajans[a] and E. Gilson
Department of Physics, University of California—Berkeley, Berkeley, California 94720-7300

L. Friedland
Racah Institute of Physics, Hebrew University of Jerusalem, 91904 Jerusalem, Israel

(Received 29 April 1999; accepted 23 August 1999)

The autoresonant (nonlinear phase locking) manipulation of the diocotron mode in a non-neutral plasma is investigated. Autoresonance is a very general phenomenon in driven nonlinear oscillator and wave systems. By sweeping or chirping the drive frequency, autoresonance allows the amplitude of a nonlinear wave to be controlled without the use of feedback. The experimental results, including a novel scaling relation, are in excellent agreement with a simple theoretical model. These are the first controlled laboratory studies of autoresonance in a collective plasma system. © *1999 American Institute of Physics.* [S1070-664X(99)02512-4]

I. INTRODUCTION

The oscillation frequency of a nonlinear, Duffing-like oscillator changes with amplitude. If you excite such an oscillator by driving it at its linear resonant frequency, the oscillator's amplitude will grow only marginally before its shifting frequency causes it to go out of phase with its drive, after which the oscillator's amplitude will beat back down to zero. By measuring the oscillator's instantaneous frequency and phase, you could use feedback to grow the oscillator's amplitude arbitrarily. But how can you grow the oscillator to high amplitude without feedback? A general property of weakly driven, nonlinear oscillators is that, under certain conditions, they *automatically* stay in resonance with their drives even if the parameters of the system vary in time and/or space. This phenomenon is called autoresonance. For example, consider an oscillator whose frequency increases with oscillation amplitude. Assume that the oscillator is initially phase locked to its drive. In autoresonance, sweeping the drive frequency upwards or downwards will cause a corresponding increase or decrease in the oscillation amplitude, so that the nonlinear frequency just matches the drive frequency.

We have demonstrated[1] autoresonance in a pure-electron plasma using the diocotron mode.[2] A detailed description of the diocotron mode follows, but for now regard the diocotron mode as a very-high-Q oscillator whose frequency increases with amplitude. Typical examples of the autoresonant excitation of this mode by a swept frequency drive are shown in Figs. 1 and 2. Autoresonance can occur for any change in the oscillator parameters, not just for a swept frequency drive. For example, if the linear frequency of the mode decreases slowly, the mode will grow autoresonantly when driven with a constant frequency (Fig. 3).

For autoresonance to occur, the mode must phaselock with the drive. Normally, phase locking occurs automatically. As shown in Fig. 4, the mode starts out unlocked to the drive, but quickly locks in. There may be substantial phase excursions, but when the mode stays phaselocked, it necessarily follows the drive frequency to high amplitude. If it loses lock, as shown for the 0.087 Vp−p curve in Fig. 4, autoresonance fails. Failure occurs only when the drive frequency or system parameters are changed too quickly or when the drive amplitude is too small. For a fixed chirp rate $\mathcal{A}$ (the change in the drive frequency per second), there is a critical drive amplitude V_a below which the maximum mode amplitude is relatively small and increases with the drive amplitude, and above which the mode amplitude follows the drive frequency to high amplitude and is independent of the drive amplitude. As shown in Fig. 5, the threshold is very sharp. Lower chirp rates have lower critical drive amplitudes. Theoretically (see Sec. IV),

$$V_a \propto \mathcal{A}^{0.75}, \tag{1}$$

and is in excellent agreement with the data, as shown in Fig. 6.

The autoresonance concept dates back to McMillan[3] and Veksler,[4] and was further developed by Bohm and Foldy[5] for particle accelerators. The term ''phase stability principle'' was used to describe the phenomenon in these early studies. The synchrotron, synchrocyclotron,[6] and other, later acceleration schemes[7,8] all are based on autoresonance. Recently, the effect has been studied theoretically in atomic and molecular physics,[9,10] nonlinear dynamics,[11,12] nonlinear waves,[13] and fluid dynamics.[14]

''Jumps'' and other hysteretic phenomena have long been studied in nonlinear dynamics.[15] The swept, or nonstationary excitation of oscillators has also been studied. The linear case was solved exactly,[16] and Mitropolskii[17] has studied the nonlinear case. None of these studies uncover the threshold and scaling effects discussed here. Entrainment in self-excited systems like van der Pol oscillators[18] bears some resemblance to the results discussed here, as do effects noted in computer modeling of planetary systems.[19]

We begin the body of this paper with a discussion of the diocotron mode. The autoresonant process naturally divides

[a]Electronic mail: joel@physics.berkeley.edu

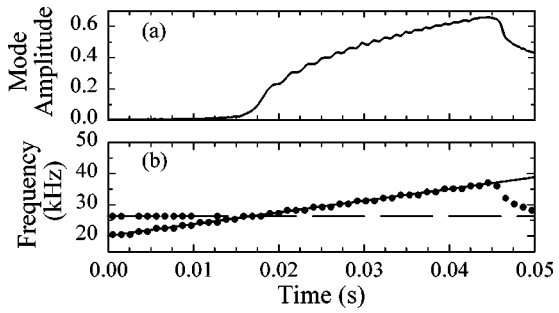

FIG. 1. Autoresonant response to a swept drive. (a) Mode amplitude D/R_w. (b) Drive frequency (solid line), measured linear resonant frequency (dashed line), and measured excitation frequencies (●). The driving frequency is swept from 20 kHz (well below the linear resonant frequency) to 45 kHz (well above the linear resonant frequency) in 0.067 s and the drive amplitude is 0.5 Vp−p. At first, the mode amplitude is small, and has frequency components at both the drive frequency and the linear diocotron mode frequency. After the drive frequency passes the linear resonant frequency, the amplitude grows autoresonantly, and only one frequency is present. Finally, the amplitude grows large enough to send the plasma into the wall, and the mode frequency drops precipitously.

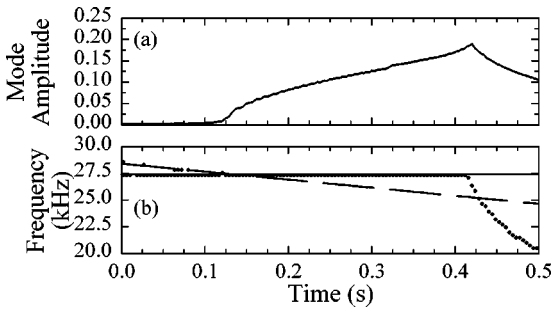

FIG. 3. Response to a constant frequency drive. Autoresonance occurs because the system's linear resonant frequency drops as the plasma expands. (a) Mode amplitude D/R_w. (b) Drive frequency (solid line), measured linear resonant frequency (dashed line), and measured excitation frequencies (●). The drive frequency is 27.4 kHz and the drive amplitude is 0.04 Vp−p. The initial linear diocotron frequency is 28.4 kHz, but plasma expansion causes the linear diocotron frequency to drop (Ref. 24) by about 14% in 0.5 s (The background residual gas pressure was deliberately set high to increase the expansion rate.) Autoresonant growth occurs only after the linear mode frequency has dropped to the drive frequency, at $t=0.11$ s.

into phase-trapping, weakly nonlinear, and strongly nonlinear regimes, and each will be discussed in turn.

II. THE DIOCOTRON MODE

The diocotron is a very basic mode in pure-electron plasmas confined in a Malmberg-Penning traps.[20] These traps consist of a series of collimated conducting cylinders immersed in a strong, axial magnetic field **B** (see Fig. 7). The plasma forms a cylindrical column inside a center cylinder. Longitudinal confinement is provided by appropriately biasing the end cylinders. Radial confinement is provided by the axial magnetic field. The **E**×**B** drifts which result from the plasma's self-electric field cause the plasma to rotate around itself (see Fig. 8). In global thermal equilibrium, the plasma rotates rigidly with frequency f_R; in the partially equilibrated plasmas used in this work the plasma's self-rotation rate is only approximately constant. If the plasma is moved off center, it undergoes an additional $\mathbf{E}_i\times\mathbf{B}$ drift from the electric field of its image. As this drift always points azimuthally, the plasma orbits around the trap center. This motion, at frequency *f*, is called the diocotron mode and is very stable, lasting for hundreds of thousands of rotations.

Assuming that the plasma column's charge per unit length is λ, the electric field of its image, E_i, is approximately radial and constant across the plasma, $E_i \approx 2\lambda D/(R_w^2-D^2)$ (cgs-Gaussian units). Here R_w is the wall radius, and D is the offset of the plasma column from the

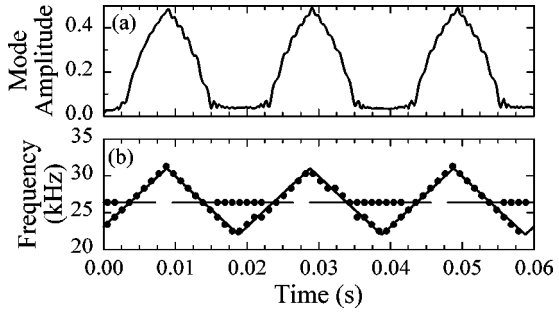

FIG. 2. Autoresonant response to a sawtooth swept drive. (a) Mode amplitude D/R_w. (b) Drive frequency (solid line), measured linear resonant frequency (dashed line), and measured excitation frequencies (●). The 1.5 Vp−p drive is repeatedly swept up and down between 22 and 31 kHz. The mode amplitude grows when the drive frequency is swept upwards, and damps when the drive frequency is swept downwards. Notice that only the drive frequency is present in the autoresonant region when the drive frequency is above the linear frequency, while the drive and the linear mode frequencies are both present when the drive frequency is below the linear frequency.

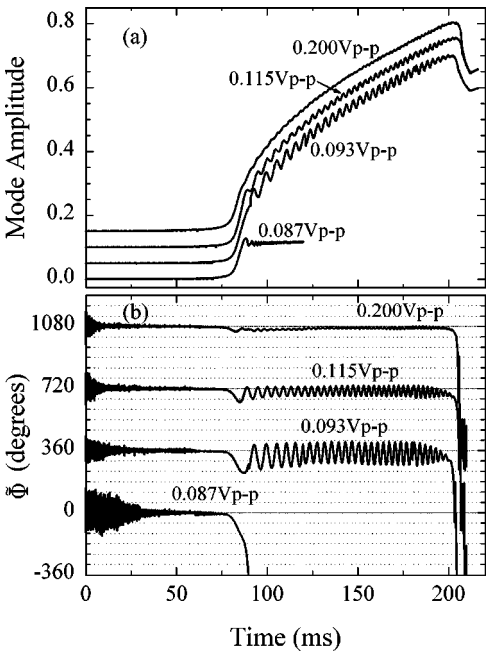

FIG. 4. (a) Mode amplitude D/R_w as a function of time for drive amplitudes of 0.087, 0.093, 0.115, and 0.200 Vp−p. (b) Mode phase relative to the drive as a function of time. Phase locking occurs in 30 ms or less. To improve visibility, the curves are displaced by 0.05 in (a) and 360 degrees in (b). The phases for $t<75$ ms are noisy because the mode amplitude is small. All data are taken at a chirp rate of $\mathcal{A}=6.8\times10^4$ Hz/s, starting at $f_{init}=20.0$ kHz.

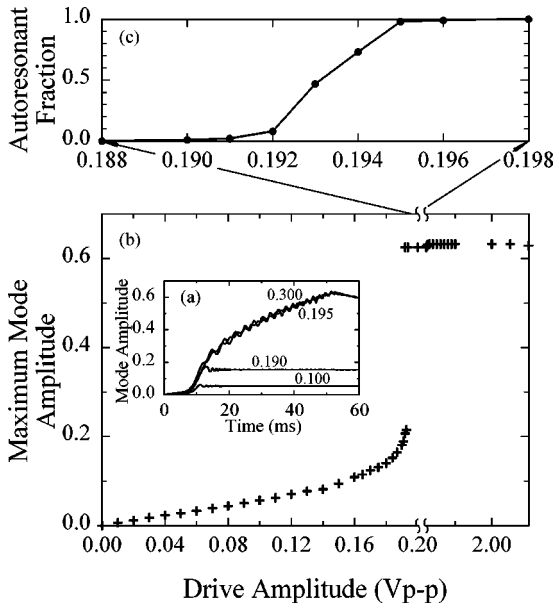

FIG. 5. Autoresonant response near threshold. (a) Mode amplitude D/R_w as a function of time for drive amplitudes of 0.100, 0.190, 0.195, and 0.300 Vp−p. Note that the response to the 0.195 and 0.300 Vp−p drives is essentially identical. (b) Maximum mode amplitude as a function of drive amplitude. Near the drive threshold voltage 0.193 Vp−p, the response is bimodal; some shots stay low, while other shots go to high amplitude. (c) The fraction of shots near threshold that go to high amplitude. All data are taken at a chirp rate of $\mathcal{A}=2\times10^5$ Hz/s.

center, i.e., the mode amplitude. The diocotron mode frequency f follows by equating $2\pi fD$ to $c\mathbf{E}_i\times\mathbf{B}/B^2$, giving

$$f=f_0\left(\frac{1}{1-D^2/R_w^2}\right), \tag{2}$$

where $f_0=\omega_0/2\pi\equiv c\lambda/\pi BR_w^2$ is the linear resonant frequency. Note that the mode frequency increases with mode amplitude.[21,22] Experimentally, we can determine both the mode frequency and amplitude by measuring the image charge at a particular angle on the trap wall as a function of time. More precisely, we measure the time dependence of the surface charge on an azimuthal sector like the one labeled V_θ in Fig. 8. The received signal is calibrated to the displacement D by imaging the plasma on the phosphor screen at the end of the trap.

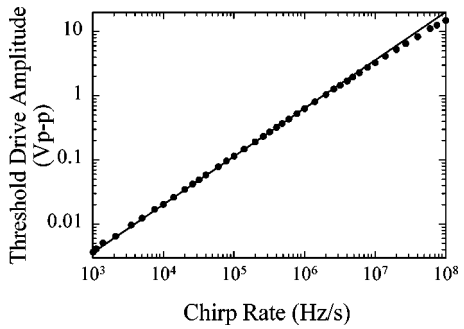

FIG. 6. Critical amplitude V_a vs. chirp rate $\mathcal{A}$. Measured results (●), and theoretical prediction from Eq. (1) (solid line). The proportionality constant in Eq. (1) is fit to the data.

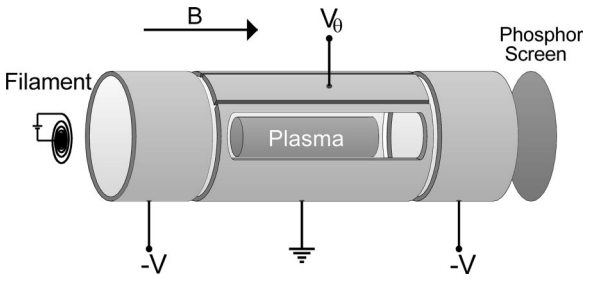

FIG. 7. Basic trap geometry. The plasma is emitted from the filament, and loaded into the trap by temporarily grounding the left cylinder. Details of the trap operation can be found in Ref. (20).

The experiments reported here were done at $B=1485$ G in a trap with wall radius $R_w=1.905$ cm. The plasma density was approximately 2×10^7 cm^{-3}, temperature $T=1$ eV, and plasma radius 0.6 cm. The measured linear diocotron frequency[23] was approximately 26.5 kHz. The plasma was confined within negatively biased cylinders separated by 10.25 cm. Finite length and radius effects, discussed in Ref. 24, increase the linear frequency from that given by Eq. (2) by approximately 40% and also modify the dependence on D. We have obtained similar autoresonance effects for plasmas of various lengths, densities, and radii, confined by magnetic fields of various strengths.

We drive the mode by applying a signal to a second, driving sector V_D.[25] This driving signal creates electric fields which induce additional drifts. As we generally use weak driving signals, these drifts are much smaller than the rotation and diocotron drifts. Nevertheless, because of phase locking, these drifts are sufficient for efficient control of the diocotron mode.

Formally, the mode obeys the following equations[26]

$$\dot{D}=-\frac{c}{BD}\frac{\partial V}{\partial\theta}, \tag{3}$$

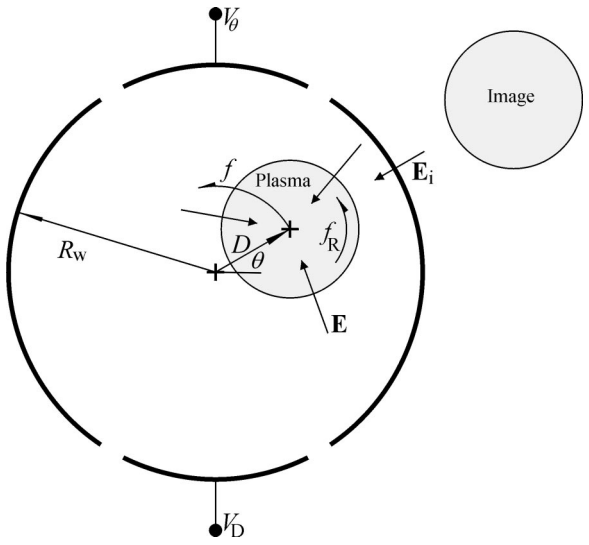

FIG. 8. Endview of the trap showing the confining wall at R_w, the pickup V_θ and drive V_D sectors, the plasma at angle θ and distance D from the trap center, the self-electric field $\mathbf{E}$, the self-rotation drift f_R, the plasma image, the image electric field $\mathbf{E}_i$, and the diocotron drift at frequency f.

$$\dot{\theta}=\frac{c}{B}\left[\frac{2\lambda}{R_w^2-D^2}+\frac{1}{D}\frac{\partial V}{\partial D}\right],$$

where the drive potential is

$$V(D,\theta,t)=\mathrm{Re}\left[\sum_{l=0}^{\infty}A_l\left(\frac{D}{R_w}\right)^l\exp[i(l\theta-\phi)]V_0\right], \qquad (4)$$

and V_0 and $\phi\equiv\int\omega(t)\,dt$ are the amplitude and phase of the drive. The A_l are the appropriate geometric factors for each l component. If we assume that the drive frequency is swept linearly, the drive frequency is

$$\omega(t)=\omega_0(t)+\alpha t, \qquad (5)$$

where $\alpha=2\pi\mathcal{A}$ is the chirp rate. To account for variations in the system parameters, we allow $\omega_0(t)$ to be a slow function of time. Usually $\omega_0(t)$ is constant, but variations in $\omega_0(t)$ can be caused by plasma expansion (as in Fig. 3), azimuthally dependent static potentials applied to the trap walls,[27] or other system manipulations.

Equation (3) is best transformed to action-angle variables. We retain only the resonant ($l=1$) term in Eq. (4), define the action $I=(D/R_w)^2$, and rewrite Eq. (3) as

$$\begin{aligned}\dot{I}&=2\epsilon I^{1/2}\sin\Phi,\\ \dot{\Phi}&=\frac{\omega_0(t)}{1-\beta I}-\omega(t)+\epsilon I^{-1/2}\cos\Phi,\end{aligned} \qquad (6)$$

where the phaseslip is $\Phi=\theta-\phi$, and $\epsilon=cA_1V_0/BR_w^2$ is the normalized drive amplitude. The factor β generalizes Eq. (3) to account for a broad class of finite length and radius corrections to the linear frequency.[24] For our experiments, β is measured to be approximately 0.60. These equations also follow from the isolated-resonance action-angle Hamiltonian for the diocotron mode[26]

$$H(I,\theta;t)=-\frac{\omega_0(t)}{\beta}\ln(1-\beta I)+2\epsilon I^{1/2}\cos(\theta-\phi). \qquad (7)$$

Note that Eqs. (6) differ from those in the classical theory of nonlinear resonance by the slow variation of ω_0 and ω with time.

III. LINEAR, PHASE-TRAPPING REGIME

Since the drive amplitude is assumed to be small, the mode is in the linear regime when the drive is first applied. Then Eq. (6) describes a driven simple harmonic oscillator (SHO):

$$\begin{aligned}\dot{I}&=2\epsilon I^{1/2}\sin\Phi,\\ \dot{\Phi}&=\omega_0(t)-\omega(t)+\epsilon I^{-1/2}\cos\Phi.\end{aligned} \qquad (8)$$

The linear regime extends from time $t_s<0$ when the drive is first applied, to roughly $t=0$ when the drive frequency equals the linear resonant frequency. Equations (8) were solved exactly in terms of Fresnel sine and cosine functions by Lewis.[16] However, the behavior of the solution can be understood quite simply. Like any SHO, the sudden application of the drive excites a driven mode at the drive frequency and an undriven, homogeneous mode at the linear frequency.

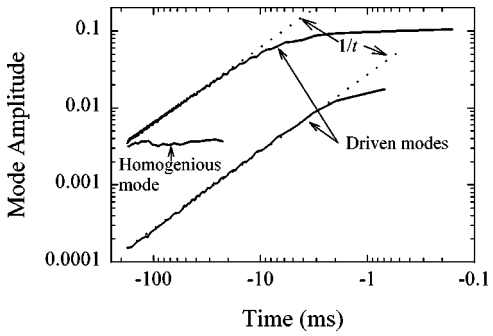

FIG. 9. Linear regime growth. The drive for the lower data, 0.050 mVp−p, is 25 times lower than the drive for the upper data. Averaging techniques used to obtain the lower data preclude measuring the homogeneous mode for this drive. All data were taken with a chirp rate of $\mathcal{A}=1.7\times10^5$ Hz/s. The initial frequency was $f_{\mathrm{init}}=15.0$ kHz.

Assuming that the net amplitude at $t=t_s$ is zero, the two modes have equal amplitude, are proportional to the drive, and inversely proportional to the deviation $\Delta\omega(t_s)=\omega(t_s)-\omega_0(t_s)=\alpha t_s$ from the linear frequency. Thereafter, just like in a steady state SHO, the amplitude of the driven mode continues to be approximately inversely proportional to $\Delta\omega(t)$. Thus the mode grows proportional to $1/t$. Remarkably, the homogeneous mode is not further excited by the sweeping frequency. This behavior is demonstrated in Fig. 9. Other experiments (not shown) have verified all the proportionalities (with α, ϵ, t_s, etc.).

The driven mode locks to the drive, while the homogeneous mode free runs. The net motion of the plasma column is the sum of the driven and homogeneous modes. Initially, the net motion will not be phaselocked to the drive because the amplitudes of the two modes are comparable. But since the driven mode amplitude grows while the homogeneous mode amplitude is constant, the driven mode will soon dominate, and the net motion will quickly phaselock. The phase locking process is easily visible in Fig. 4(b). The occurrence of automatic phase locking is not self-evident, as the system, in a Hamiltonian picture, has to cross the separatrix between streaming and trapped orbits.

IV. WEAKLY NONLINEAR REGIME

Near $t=0$, the mode grows out of the linear regime and stops increasing like $1/t$. Retaining the first nonlinear correction to the frequency in Eq. (6) yields

$$\dot{I}=2\epsilon I^{1/2}\sin\Phi, \qquad (9)$$

$$\dot{\Phi}=\omega_0(1+\beta I)-\omega+\epsilon I^{-1/2}\cos\Phi, \qquad (10)$$

where we have suppressed the time dependencies in ω_0 and ω. Assuming that these frequencies are slowly varying, we write $I=I_0+\Delta$; the action oscillates with quickly-varying amplitude $\Delta(t)$ around the slowly evolving average action $I_0(t)$. By further assuming that Δ is small, and $\Phi=\pi+\tilde{\Phi}$, Eq. (10) simplifies to

$$\dot{\tilde{\Phi}}=\left(\beta\omega_0+\frac{\epsilon}{2I_0^{3/2}}\cos\tilde{\Phi}\right)\Delta-\alpha t+\beta\omega_0 I_0-\frac{\epsilon}{I_0^{1/2}}\cos\tilde{\Phi}. \qquad (11)$$

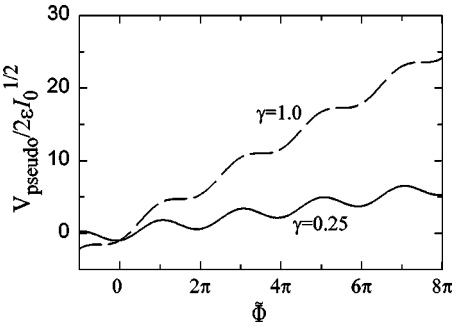

FIG. 10. Critical (dashed line) and typical above-threshold (solid line) normalized pseudopotentials $V_{\text{pseudo}}/2\epsilon I_0^{1/2} = -\cos\tilde{\Phi} + \gamma\tilde{\Phi}$ as a function of the phaseslip $\tilde{\Phi}$, where $\gamma = (\alpha - \beta\dot{\omega}_0 I_0)/2\epsilon I_0^{1/2} S$. The critical pseudopotential is defined by Eq. (19); i.e., $\gamma = 1.0$. The particular above threshold pseudopotential drawn here is defined by $\gamma = 0.25$.

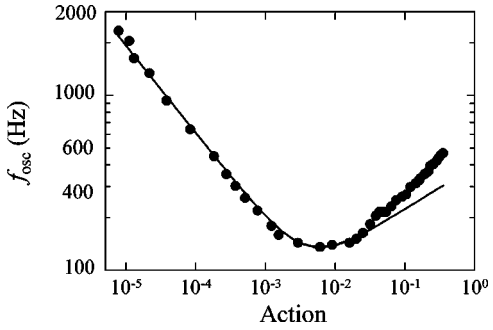

FIG. 11. Action versus pseudoparticle oscillation frequency. The dots are measured experimentally, and the line plots $f_{\text{osc}} \propto \sqrt{I_0^{1/2} S}$, where the position of the minimum and the frequency at the minimum are fit to the data. The drive amplitude was 0.15 Vp−p. The discrepancy between the experiment and theory at large action is due to the supralinear terms in the nonlinear frequency [Eq. (2)], which are not included in the weakly nonlinear theory.

Next, we assume that $\tilde{\Phi}$ is small, and set $\cos\tilde{\Phi} \approx 1$ in this equation. We define $I_0(t)$ by setting the last three terms on the right-hand side to zero:

$$-\alpha t + \beta\omega_0 I_0(t) - \frac{\epsilon}{I_0(t)^{1/2}} = 0. \tag{12}$$

This is equivalent to defining $I_0(t_0)$ to be equal to the steady-state excitation amplitude for a drive of amplitude ϵ and constant drive frequency $\omega_0 + \alpha t_0$. Using Eq. (12), Eq. (11) reduces to

$$\ddot{\tilde{\Phi}} = S\Delta, \tag{13}$$

where the slowly varying parameter S is

$$S = \beta\omega_0 + \frac{\epsilon}{2I_0^{3/2}}. \tag{14}$$

Differentiating Eq. (12) and solving for $\dot{I}_0$ yields

$$\dot{I}_0 = \frac{\alpha - \beta\dot{\omega}_0 I_0}{\beta\omega_0 + \epsilon/2I_0^{3/2}} = \frac{\alpha - \beta\dot{\omega}_0 I_0}{S}. \tag{15}$$

This expression can be used to evaluate $\dot{\Delta} = \dot{I} - \dot{I}_0$. To lowest order,

$$\dot{\Delta} = -2\epsilon I_0^{1/2}\sin\tilde{\Phi} - \frac{\alpha - \beta\dot{\omega}_0 I_0}{S}. \tag{16}$$

Together Eqs. (13) and (16) form a Hamiltonian system with

$$H(\tilde{\Phi}, \Delta) = S\Delta^2/2 + V_{\text{pseudo}}(\tilde{\Phi}), \tag{17}$$

where

$$V_{\text{pseudo}}(\tilde{\Phi}) = -2\epsilon I_0^{1/2}\cos\tilde{\Phi} + \frac{\alpha - \beta\dot{\omega}_0 I_0}{S}\tilde{\Phi}. \tag{18}$$

The potential, V_{pseudo}, looks like a tilted series of potential wells (see Fig. 10). Consequently, the system reduces to a pseudoparticle of slowly varying mass S^{-1} moving in a slowly varying pseudopotential V_{pseudo}.

The initial phase trapping regime traps the pseudoparticle into the pseudopotential. Once trapped, the pseudoparticle will tend to stay trapped so long as (1) its mass S^{-1} and the pseudopotential vary slowly, and (2) the pseudopotential wells continue to exist. Translated back to the original system, the diocotron mode amplitude will stay locked to drive frequency [through Eq. (12)] so long as the pseudoparticle is trapped.

We tested the above model by measuring the small-amplitude oscillation frequency of the pseudoparticle in the well, $\omega_{\text{osc}} = 2\pi f_{\text{osc}} = \sqrt{2\epsilon I_0^{1/2} S}$ [derived by ignoring the $\alpha - \beta\dot{\omega}_0 I_0$ term in Eq. (18).] The pseudoparticle oscillations manifest themselves as the amplitude and phase oscillations in Fig. 4. Experimentally, f_{osc} scales appropriately with ϵ (data not shown). More interesting is the dependence of f_{osc} on the action I_0; f_{osc} has a minimum at an intermediate value of the action (see Fig. 11). The pseudopotential wells are at their shallowest at this minimum, and, taking into account the linear term $[(\alpha - \beta\dot{\omega}_0 I_0)\tilde{\Phi}/S]$ in the pseudopotential, are in danger of disappearing altogether. Indeed, $dV_{\text{pseudo}}/d\tilde{\Phi}$ must be negative at some phase $\tilde{\Phi}$ for the wells to exist. Thus, from Eq. (18)

$$2\epsilon I_0^{1/2} > \frac{\alpha - \beta\dot{\omega}_0 I_0}{S}. \tag{19}$$

Rewriting,

$$2\epsilon I_0^{1/2} S = \omega_{\text{osc}}^2 > \alpha - \beta\dot{\omega}_0 I_0. \tag{20}$$

The minimum in ω_{osc} occurs when $d(I_0^{1/2}S)/dI_0$ equals zero, at the critical action $I_{0\text{crit}} = (\epsilon/\beta\omega_0)^{2/3}$. Using $I_{0\text{crit}}$ to evaluate the minimum value of $I_0^{1/2}S$ yields the minimum oscillation frequency $\omega_{\text{osc min}}^2 = 3(\beta\omega_0)^{2/3}\epsilon^{4/3}$. Thus, condition (20) is always satisfied only when the drive amplitude exceeds

$$\epsilon > \frac{1}{\sqrt{\beta\omega_0}}\left(\frac{\alpha - \beta\dot{\omega}_0 I_0}{3}\right)^{3/4} \equiv \epsilon_a. \tag{21}$$

Above this critical value the pseudopotential has wells, while below the wells disappear. Note that (ignoring the $\beta\dot{\omega}_0 I_0$ term) this condition is identical to the threshold scaling law Eq. (1).

For most system parameters, $I_{0\text{crit}}$ is quite small. For ϵ near the critical value [Eq. (21)], $I_{0\text{crit}}$ is approximately

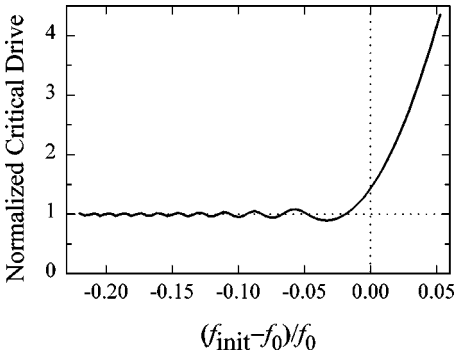

FIG. 12. Experimentally determined critical drive amplitude as a function of $(f_{\rm init}-f_0)/f_0$, where $f_{\rm init}$ is the drive frequency at the beginning of the sweep. The drive amplitude is normalized to unity at large $-(f_{\rm init}-f_0)/f_0$, and $\mathcal{A}=1.5\times10^6$ Hz/s.

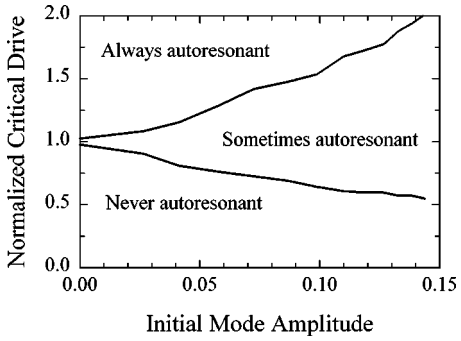

FIG. 13. Experimentally determined critical drive amplitude as a function of the amplitude $D/R_{\rm w}$ of the diocotron mode just before the sweep begins. The parameter space is divided into the three regions indicated on the figure. In the ''sometimes autoresonant'' region, an individual experimental shot will be autoresonant or not depending on the random phase relationship between the preexisting mode and the drive. The critical drive amplitude is normalized to one at zero initial mode amplitude. For this data, $\mathcal{A}=1.5\times10^6$ Hz/s, and $f_{\rm init}=15.0$ kHz.

$3^{-1/2}(\beta\omega_0)^{-1}(\alpha-\beta\dot{\omega}_0 I_0)^{1/2}$, which is indeed small for any reasonable chirp rate. Most of this discussion assumes a chirping drive frequency $[\dot{\omega}(t)<0]$ and a constant linear mode frequency $[\dot{\omega}_0(t)=0]$, yielding $\alpha\neq0$. When the drive frequency is constant $[\dot{\omega}(t)=0]$ and the linear mode frequency droops $[\dot{\omega}_0(t)<0]$, by Eq. (5), α is still nonzero, namely $\alpha=-\dot{\omega}_0(t)$. Because $I_{0\rm crit}$ is small, the α term will dominate the $\beta\dot{\omega}_0 I_0$ term in Eq. (21) and the threshold condition will remain essentially unchanged.

In summary, autoresonance will occur when the drive amplitude exceeds the critical value given in Eq. (21). As shown in Fig. 4, the trapping oscillations start small (after the initial trapping period), reach a maximum at a mode amplitude corresponding to $I_{0\rm crit}$, and then, assuming that detrapping does not occur, diminish. When the drive amplitude is well above critical value, the pseudoparticle is deeply trapped and the trapping oscillations are small. But when the drive amplitude approaches the critical value, the trapping oscillations grow to almost 180°. When the oscillations exceed 180° the pseudoparticle escapes by rolling out of the now-vanished pseudopotential wells, and autoresonance fails. Since $I_{0\rm crit}$ is small, the autoresonant behavior is determined at low mode amplitude. When autoresonance fails, it fails at low amplitude; when it succeeds, it grows well beyond $I_{0\rm crit}$, thereby explaining the sharp threshold observed in Fig. 5.

The critical threshold condition [Eq. (21)] is exact only when the system reaches the critical action $I_{0\rm crit}$ with little initial oscillation amplitude. If the frequency sweep is started too close to the linear frequency ω_0 (Fig. 12), or if the mode is already excited before the sweep begins (Fig. 13), the threshold condition changes. Sometimes the initial oscillation lowers the critical drive amplitude, and sometimes it increases the critical drive amplitude, but in all cases the change is surprisingly small.

Finite length and self-shielding effects make it difficult to calculate the geometric factor A_1 required to relate the threshold drive voltage $V_{\rm a}$ and $\epsilon_{\rm a}$ in Eq. (21). Nevertheless, the calibration can be found indirectly by expressing $V_{\rm a}$ in terms of the measured minimum pseudopotential oscillation frequency $\omega_{\rm osc\,min}$. One finds

$$V_{\rm a}=\frac{V_{\rm osc}}{\omega_{\rm osc\,min}^{3/2}}\alpha^{3/4}, \tag{22}$$

where $V_{\rm osc}$ is the drive voltage used to obtain the oscillation frequency curve. Using the data in Fig. 11, $V_{\rm osc}=0.15\,{\rm Vp-p}$ and $\omega_{\rm osc\,min}/2\pi=136\,{\rm Hz}$, yields $V_{\rm a}=2.38\times10^{-5}\mathcal{A}^{3/4}$, about 15% higher than the experimental value (from Fig. 6) of $V_{\rm a}=(2.05\pm.05)\times10^{-5}\mathcal{A}^{3/4}$. Note that numerical simulations typically find thresholds within 10% of the value predicted by Eq. (21).

V. STRONGLY NONLINEAR REGIME

In the strongly nonlinear regime, the action approaches one, and the $\epsilon I^{-1/2}\cos\Phi$ term in Eq. (6) can be neglected. Defining the slowly varying average action via

$$\frac{\omega_0(t)}{1-\beta I_0(t)}-\omega(t)=0 \tag{23}$$

and using $I=I_0+\Delta$ allows us to transform Eq. (6) to

$$\dot{\Delta}\approx-2\epsilon I_0^{1/2}\sin\tilde{\Phi}, \tag{24}$$

$$\dot{\tilde{\Phi}}\approx\frac{\beta\omega_0(t)}{(1-\beta I_0)^2}\Delta, \tag{25}$$

or

$$\ddot{\tilde{\Phi}}=-2\epsilon\beta\omega_0\frac{I_0^{1/2}}{(1-\beta I_0)^2}\sin\tilde{\Phi}. \tag{26}$$

Thus small oscillations around the slowly varying average action I_0 have frequency $\omega_{\rm osc}^2=2\epsilon\beta\omega_0 I_0^{1/2}/(1-\beta I_0)^2$. If the amplitudes of these oscillations of Δ and $\tilde{\Phi}$ are δI and $\delta\tilde{\Phi}$, then, from Eq. (24), $\omega_{\rm osc}\delta I=2\epsilon I_0^{1/2}\delta\tilde{\Phi}$. For the system to stay locked, we require $\delta\tilde{\Phi}<\pi$, while $\delta I/I_0\ll1$ for the validity of our expansion procedure. On the other hand, the product $\delta\tilde{\Phi}\,\delta I=J$ remains constant under adiabatic conditions, so we must have simultaneously

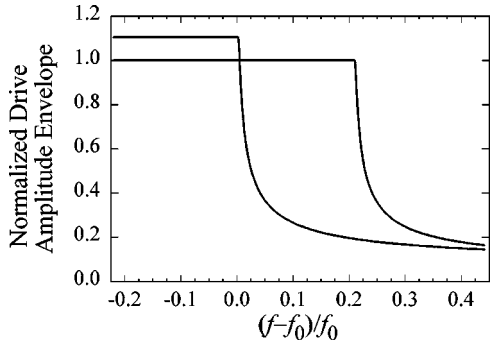

FIG. 14. Two autoresonant drive amplitude envelopes that experimentally yield autoresonance. The drive frequencies are scaled to the linear resonant frequency f_0. The standard minimum [Eq. (21)] autoresonant drive envelope is independent of frequency, and, with the normalization used in this graph, would have value one. Autoresonance will still occur if, as the drive frequency is swept upwards, the drive amplitude is decreased according to either of the two envelopes shown. Other envelopes will also work so long as their amplitude in the vicinity of the critical action (just above f_0) is greater or equal to one.

$$\frac{\delta I}{I_0}=\frac{[J(1-\beta I_0)]^{1/2}}{I_0^{7/8}}\left(\frac{2\epsilon}{\beta\omega_0}\right)^{1/4}\ll 1 \tag{27}$$

and

$$\delta\tilde{\Phi}=\frac{J^{1/2}}{I_0^{1/8}(1-\beta I_0)^{1/2}}\left(\frac{2\epsilon}{\beta\omega_0}\right)^{-1/4}<\pi. \tag{28}$$

By combining these two inequalities,

$$\frac{J^2}{\pi^4 I_0^{1/2}(1-\beta I_0)^2}<\frac{2\epsilon}{\beta\omega_0}\ll\frac{I_0^{7/2}}{[J(1-\beta I_0)]^2}. \tag{29}$$

Note that if satisfied initially, the right inequality in Eq. (29) improves continuously as I_0 grows in autoresonance. The left inequality also improves until $\beta I_0=0.2$, or [see Eq. (23)] until $(f-f_0)/f_0=\beta I_0/(1-\beta I_0)=0.25$. Consequently, in the strongly nonlinear regime, the drive amplitude can be lower at high mode amplitude than at low mode amplitude. This counter-intuitive phenomenon is illustrated in Fig. 14.

VI. CONCLUSIONS

Autoresonance is a powerful technique for controlling the amplitude of nonlinear modes. It is a robust method because, over a broad range of parameters, it does not depend on the details of the system, nor on the amplitude or exact range of the sweeping drive. It is insensitive to any initial noise. To the best of our knowledge, the amplitude-chirp rate scaling law [Eq. 21)] is novel to plasma physics and to nonlinear dynamics. As with autoresonance in general, the scaling law does not depend on the details of the system.

The data reported here were all taken at Q's of approximately 10^5. While we have observed autoresonant phenomenon in diocotron systems with Q's as low as 60, too low a Q suppresses autoresonance. Not surprisingly, damping suppresses autoresonance more readily at low drive amplitude. The effects of intermediate Q values include an upward shift of the critical action, and a reduced amplitude jump at the threshold. As the system is no longer Hamiltonian, our theoretical analysis is no longer strictly valid and more sophisticated techniques must be employed. However, when Q is sufficiently low, the chirp rate sufficiently small, and the drive sufficiently large, Mitropolskii's analysis[17] becomes relevant.

Our theoretical analysis assumes that the oscillator's nonlinear frequency shift scales as the amplitude squared, but since the critical amplitude is low, higher-order corrections are unimportant. Thus, the results extend beyond the Duffing equation $[f(D)=f_0(1+\beta D^2)]$ to the driven pendulum equation, the diocotron mode $[f(D)=f_0/(1-\beta D^2)]$, and many other driven nonlinear systems.

ACKNOWLEDGMENTS

The authors thank the Office of Naval Research and the Binational U.S.–Israel Science Foundation for funding this project, and Professor J. S. Wurtele for his helpful comments.

[1] J. Fajans, E. Gilson, and L. Friedland, Phys. Rev. Lett. **82**, 4444 (1999).
[2] W. D. White, J. H. Malmberg, and C. F. Driscoll, Phys. Rev. Lett. **49**, 1822 (1982).
[3] E. M. McMillan, Phys. Rev. **68**, 143 (1945).
[4] V. Veksler, J. Phys. (USSR) **9**, 153 (1945).
[5] D. Bohm and L. Foldy, Phys. Rev. **70**, 249 (1946).
[6] M. S. Livingston, *High-Energy Particle Accelerators* (Interscience, New York, 1954).
[7] K. S. Golovanivski, IEEE Trans. Plasma Sci. **PS-11**, 28 (1983).
[8] L. Friedland, Phys. Plasmas **1**, 421 (1994).
[9] B. Meerson and L. Friedland, Phys. Rev. A **41**, 5233 (1990).
[10] W. K. Liu, B. Wu, and J. M. Yuan, Phys. Rev. Lett. **75**, 1292 (1995).
[11] B. Meerson and S. Yariv, Phys. Rev. A **44**, 3570 (1991).
[12] G. Cohen and B. Meerson, Phys. Rev. E **47**, 967 (1993).
[13] L. Friedland, Phys. Rev. E **58**, 3865 (1998), and references therein.
[14] L. Friedland, Phys. Rev. E **59**, 4106 (1990).
[15] E. V. Appelton, Philos. Mag. **47**, 609 (1924).
[16] F. M. Lewis, Trans. ASME **54**, 253 (1932).
[17] Y. A. Mitropolski, *Nonstationary Processes in Nonlinear Oscillatory Systems* (Izd-vo AN, Kiev, USSR, 1955), in Russian.
[18] T. Klinger, F. Greiner, A. Rohde, A. Piel, and M. E. Koepke, Phys. Rev. E **52**, 4316 (1995).
[19] Jack Wisdom, private communication, 1998.
[20] J. H. Malmberg, C. F. Driscoll, B. Beck, D. L. Eggleston, J. Fajans, K. Fine, X. P. Huang, and A. W. Hyatt, in *Nonneutral Plasma Physics*, edited by C. Roberson and C. Driscoll (American Institute of Physics, New York, 1988), Vol. AIP 175, p. 28.
[21] S. A. Prasad and J. H. Malmberg, Phys. Fluids **29**, 2196 (1986).
[22] K. S. Fine, Phys. Fluids B **4**, 3981 (1992).
[23] The experiments reported here were taken at slightly different trap parameters than the experiments reported earlier in Ref. 1. These differences, together with long term drifts in the trap, account for the slight differences in the reported frequencies and critical drives.
[24] K. S. Fine and C. F. Driscoll, Phys. Plasmas **5**, 601 (1998).
[25] In the experiment the receiving and driving sectors do not extend the full length of the plasma, and are separated axially to reduce coupling.
[26] R. Chu, J. S. Wurtele, J. Notte, A. J. Peurrung, and J. Fajans, Phys. Fluids B **5**, 2378 (1993).
[27] Such potentials can cause the diocotron frequency to go up or down, change the sign of nonlinear frequency dependence, and have other curious effects. A study of these effects, in the context of bifurcations in elliptical plasmas, will be published.